

MIXED ALKALI EFFECT ON STRUCTURE AND OPTICAL PROPERTIES OF QUATERNARY B_2O_3 - P_2O_5 - Li_2O -CAO GLASS CONTAINING Fe_2O_3

M. S. ABD EL KERIEM

Department of Physics, Faculty of Science, AIN Shams University, Abbasia, Cairo, Egypt

ABSTRACT

Series of alkali borophosphate glasses containing Fe_2O_3 is prepared by the conventional melt-quenching technique. The alkali mixed effect on the glass structure and its optical properties is studied through replacing Li_2O (alkali oxide) by CaO (alkaline-earth oxide). Positron spectroscopy revealed a periodic change in both the glass refractive indices and free volume size as the molar ratio of Li_2O increases. It is an evidence for a variation of nonbridging oxygen bonds (NBO) density. The molar polarizability of NBO explains the obtained optical properties, while the variation in the glass molar volume clarifies the detected variation in the glass free volume. FT-IR spectroscopy of the investigated glasses confirmed the variation in the relative NBO density as Li_2O content increases on the expense of CaO .

KEYWORDS: Mixed Alkali Effect on Structure and Optical Properties, Alkali Borophosphate, Fe_2O_3 , Li_2O , CaO

INTRODUCTION

Due their low melting temperature, high thermal expansion, wide ultraviolet transparency and low dispersion compared with silicate glasses, phosphate glasses are of great interest for various optical applications such as optical fibers [1]. Employ of phosphate glasses as achromatic host materials in solid state lasers depends on types of dopants and their concentrations [2]. However, the use of phosphate glasses in solid state lasers was limited by their low chemical durability [3].

The basic building blocks of phosphates are the P-tetrahedra which link through covalent bridging oxygens to form various phosphate anions ($v\text{-}P_2O_5$). The addition of trivalent cations into metaphosphate (ratio of O/P = 3.0) glasses can lead to an increase in the degree of structure connectivity through the substitute of P=O nonbridging bonds by bridging bonds [4]. For that reason, B_2O_3 is added in the form of BO_4 tetrahedra into phosphate glasses to improve their chemical durability providing more three-dimensional cross-linked structures [5-8]. On the other hand, borates are of exceptional importance due to their interesting linear and nonlinear optical properties [9-11]. Borophosphate glasses exhibit flat gain broadband amplification [12]. In addition, alkali-earthed-borophosphate glass matrices are of interest for many applications such as hosts for rare-earth dopants for fiber amplifiers [13]. Also, alkali-borophosphate glass exhibits large electro-optical Kerr-like effect and so large third-order nonlinearity [14, 15]. Addition of B_2O_3 to a phosphate glass improves the chemical durability as well as thermal and mechanical stability of the pure phosphate glass [16-19]. Fe_2O_3 has excellent effect on chemical durability in phosphate glass systems. The good chemical durability of the iron phosphate glass was attributed to a large number of Fe-O-P bonds in the structure [20]. Addition of iron to borate glass makes it electrically semiconducting [21]. Phosphate glasses containing divalent iron cations exhibit interesting semiconducting properties, magneto-optical properties, magnetic transition properties and electro-optic devices [22, 23].

As functions of Fe_2O_3 content, iron ions exist in different valence states with different local symmetries in the glass matrices. For example, iron ions exist as Fe^{3+} with both tetrahedral and octahedral coordination, and/or as Fe^{2+} with octahedral coordination. Both of Fe^{3+} and Fe^{2+} are paramagnetic ions [24]. The coexistence of two valence states of iron leads to interesting semiconducting and magnetic properties for iron phosphate glasses [25].

Several glasses exhibit a linear-like behavior of their physical properties with varying chemical composition. An exception exists for glasses containing two different alkali oxides where large deviation from linearity occurs having maxima or minima. The mixed alkali effect (MAE) was observed for instance as nonlinear variation in electrical conductivity isotherms when a fraction of one type of the mobile ions is replaced by another type, keeping the total alkali content constant [26]. In this work the mixed alkali effect is used to study maxima for refractive index and minima in positron lifetime are studied with the prepared glasses.

EXPERIMENTAL

Glass Preparation

Series of borophosphate glass containing iron oxide of the composition $(0.3\text{B}_2\text{O}_3 - 0.3\text{P}_2\text{O}_5 - 0.2\text{Fe}_2\text{O}_3 - x\text{Li}_2\text{O} - (0.2 - x)\text{CaO})$ with $0 \leq x \leq 0.2$ mol fraction is prepared. The used materials are of chemically pure grade, in the form of Fe_3O_4 , H_3BO_3 , CaO , $2[\text{NH}_4\text{H}_2\text{PO}_4]$ and Li_2CO_3 . The amount of the glass batch is 50 g melt^{-1} . The glass is prepared by melt quenching technique using platinum 2% rhodium crucibles in an electric furnace. The batch was pre-heated at $500\text{--}600^\circ\text{C}$ for almost an hour to evaporate the carbonates. The temperature of melting is $1000\text{--}1100^\circ\text{C}$, the duration of melting is one hour after the last traces of batches are disappeared.

To avoid the presence of bubbles the glasses are continue stirred during the glass melt preparation. Then the melt is poured onto stainless steel mould and annealed at around 350°C to remove the thermal strains. Optical slabs are prepared by grinding and polishing of the prepared samples with paraffin oil and minimum amount of water. The thickness of the glass slabs is about 3 mm. Polishing method is completed with stannic oxide and paraffin to reach a surface roughness less than $\lambda/3$, which is tested by interferometric method. The homogeneity of the glasses is examined using two crossed polarizers.

Spectrophotometric Measurements

Computer aided two-beam spectrophotometer (shimadzu-3101PC UV-VIS NIR) is used to record the reflectance, R , and the transmittance, T , data of plane-parallel polymeric film samples, A resolution limit of 0.2 nm and a sampling interval of 2 nm are utilized for the different measuring points, The accuracy of measuring $R(\lambda)$, and $T(\lambda)$ is 0.003 with the incident beam making an angle of $5.0^\circ \pm 0.1^\circ$ to the normal to external slab faces. The measurements are carried out at room temperature for the entire spectral range $0.2\text{--}2.5 \mu\text{m}$. The different optical applications of the glass require information about glass refractive index and its dispersion [9]. Applying Fresnel's theory, the glass refractive index, n , is determined by means of an iteration technique [27] using the transmittance and reflectance recorded data. The estimated uncertainty in the index of refraction is ± 0.005 .

Positron Annihilation Measurements

Positron annihilation measurements are carried out at room temperature for the investigated glass samples. The PAL spectra are recorded using a fast-fast coincidence system with a time resolution of 250 picoseconds (ps). The

positron source is prepared by drying a droplet of ²²NaCl aqueous solution (about 20μCi) on a thin kapton foil. The positron source is sandwiched between two similar samples that are each about 1 mm thick; the two samples included in the positron source are put it between the two detectors of the positron lifetime set-up.

With the emission of a positron, the source emits a γ-quantum, a photon that is recorded on one detector. A γ- ray is emitted if an electron and its antiparticle, the positron, meet and annihilate, and one of the annihilation photons is recorded on another detector. The time difference between the two signals from the two detectors is, consequently, the positron lifetime. With a suitable electronics set-up, this time difference is transformed into what is called the lifetime spectra.

The lifetime spectrum shows a curve, which is a decaying exponential, containing many components due to several annihilation processes. The area under one component divided by the total area of the spectrum is called the relative intensity (*I*) of the component. A positron can annihilate through different processes, each of which gives rise to a certain mean lifetime (τ). The analyses of the positron annihilation lifetime spectra are performed using the PATFIT program [28], which gives the average of the lifetimes and their intensities. The positron lifetime technique is discussed elsewhere [28-30].

FT-IR Vibrational Absorption Measurements

Infrared vibrational absorption measurements are recorded for the present glass compositions in the range of (1400 - 400 cm⁻¹) using Jasco FT/IR-300E infrared spectrophotometer. The alkali halide disc-technique at room temperature is used. Well-dried and ground glasses are mixed with well-dried infrared grade potassium bromide and then sufficiently ground to obtain a homogeneous mixture of minimum particle size. The mixture is mechanically pressed at 70-Mpa pressure in the form of discs.

RESULTS AND DISCUSSIONS

Dispersion Properties of Investigated Glasses

Figure 1 illustrates the calculated dispersion of refractive indices in a spectral range from 0.2 to 2.5 μm. An alternative change in the glass dispersion is seen as the ratio of Li₂O/CaO increases. At percentage of relative molar ratio of Li₂O/CaO = 25 % the glass refractive index increases $n_d = 1.8604$, as shown in Fig. 2. The refractive index, n_d , is measured at the standard wavelength $\lambda = 587.6$ nm. At percentage of relative molar ratio of Li₂O/CaO = 50 %, the glass refractive indices starts to increase having $n_d = 1.9396$. Moreover, decrease in glass refractive index is seen with sample 3 reaching $n_d = 1.9056$ at percentage of relative molar ratio of Li₂O/CaO = 75 %. With no contribution from CaO in the glass structure, i.e., at a percentage for the relative molar ratio of Li₂O/CaO = 100 % the refractive index increased once again reaching $n_d = 1.9335$. Such alternation in the glass index is attributed to an fluctuation in oscillator strength value, f_{ij} .

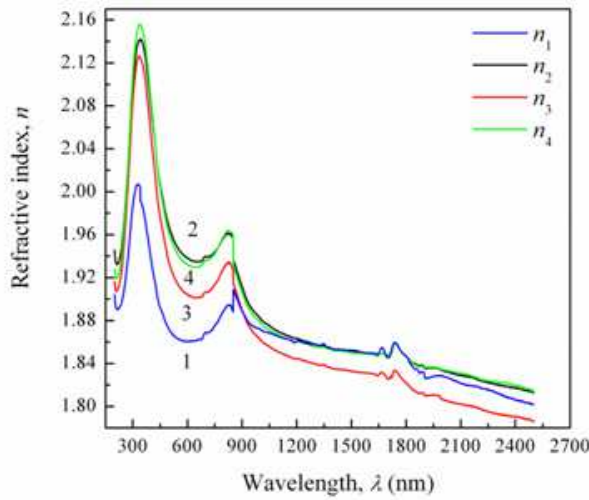


Figure 1: Dispersion of Glass Refractive Indices against Wavelength

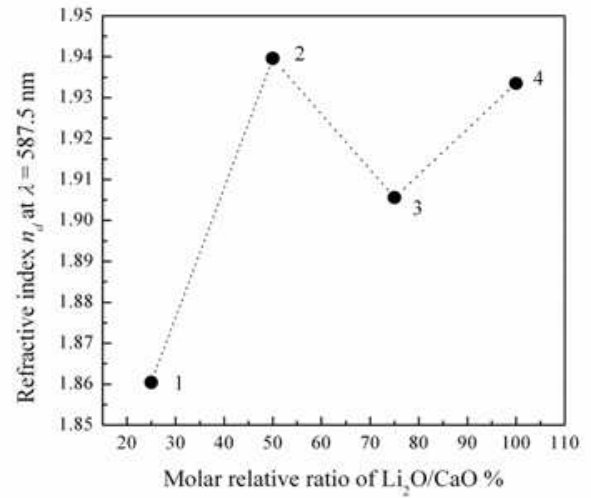


Figure 2: Variation of Glass Refractive Indices at $\lambda = 587.6$ nm versus the Percentage of Molar Ratio of $\text{Li}_2\text{O}/\text{CaO}$

As it will be seen later from the FT-IR spectroscopy, addition of a modifier oxides to borate and phosphate networks has differing effects on the glass network and hence on alternation of the glass characteristics. The basic units of pure amorphous borate glasses are trigonal BO_3 groups, whereas the basic units of pure amorphous phosphate glasses are PO_4 tetrahedra linked through covalent bridging oxygens. In case of borate network, the addition of a modifier oxide increases the degree of polymerization because the neutral trigonal $\text{BO}_{3/2}$ groups are converted to tetrahedral $\text{BO}_{4/2}^-$ species owing to Lewis acid character of boron oxide. Whereas in the phosphate network, the addition of a modifier oxide has a depolymerizing effect; the extra oxygen atoms introduced by the modifier oxides form negative nonbridging oxygen (NBO) sites, whose charge is compensated by the positive charge of the modifier cations [31].

In short, the density alternation of NBO bonds (that have high electronic oxide ion polarizability, α_{O}^{2-}) will lead to such recorded wavering in the glass refractive index values. The alternation can be more understood by reference to Lorentz-Lorenz equation [32] where:

$$\alpha_m = \frac{3M}{4\pi DN_A} \frac{(n^2 - 1)}{(n^2 + 2)} \quad (1)$$

where α_m is the molar polarizability, M is the molar mass of glass composition, D is the glass density and N_A is the density of oscillators (Avogadro's number). Furthermore, the electronic oxide ion polarizability α_{O}^{2-} is function of the molar polarizabilities and which can be considered by the following equation:

$$\alpha_{\text{O}}^{2-} = (\alpha_m - \sum_i N_i \alpha_i) / N_{\text{O}} \quad (2)$$

where N_{O} and N_i are the numbers of oxygen ions and cations, respectively. Here α_i is the electronic polarizabilities of a cation. The values of N_{O} and N_i can be obtained from chemical compositions. Thus, as the ratio of $\text{Li}_2\text{O}/\text{CaO}$ in the studied glasses composition changes the electronic polarizability of the oxygen ion changes as well describing the obtained

behavior of the glass refractive index.

Duffy et al. [33, 34] proposed the concept of optical basicity which permits a comparison of the acid-base character of oxides. The optical basicity, A , of an oxidic medium, is the average electron donor power of all the oxide atoms comprising the medium. Increasing basicity results in increasing the negative charge on the oxygen atoms and, accordingly, increasing covalency in the oxygen-cation bonding. The oxygen (oxide ion) polarizability expresses the degree of negative charge on oxygen atoms while optical basicity is a measurement of this charge [8, 35]. The intrinsic relationship between the optical basicity of the oxide medium and the electronic polarizability of the oxide ion as follows [36]:

$$A = 1.67 \left(1 - \frac{1}{\alpha_O^{2-}} \right) \quad (3)$$

An increase in the oxide ion polarizability (due to NBO that impinge on the cation species) leads to an increase in density of the negative charges on the oxygen atoms in the studied glass system and accordingly an increase in glass index.

Positron Annihilation Spectroscopy

In positron annihilation lifetime, the best fit is obtained for three-component analysis of the PAL spectra. The value of positron lifetime τ distinguishes the different types of defects. The nonbridging oxygen (NBO) associated with metal cations is considered to have a high electron density than the bridging oxygen [37, 38]. A value in the range of 200–400 ps belongs to bulk and dislocations such as NBOs [39–41]. NBO may be represented as a center of negative charge with a high electron density [37]. The long-lived component τ_3 is due to the pick-off annihilation of the o-Ps in the free-volume holes of different sizes. On the other hand, the intensity, I_3 , is proportional to the number of these free-volume holes.

According to Tao–Eldrup model [42], knowledge of the o-Ps lifetime, τ_3 , allows obtaining the average radius, R , of the nano-holes, in spherical approximation as:

$$\tau_3 = 0.5 \left[1 - \frac{R}{R + \Delta R} + \frac{1}{2\pi} \sin\left(\frac{2\pi R}{R + \Delta R}\right) \right]^{-1} \quad (4)$$

τ_3 in the range of nanoseconds is related to the existence of free volume, and $\Delta R = 0.1656$ nm is the thickness of the homogeneous electron layer in which the positron annihilates [43]. Also, the average size of the o-Ps hole volume $V_f = 4\pi R^3/3$.

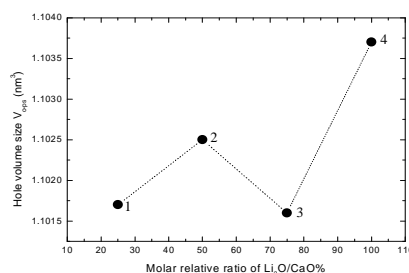


Figure 3: Variation of Free Volume against the Percentage of Molar Ratio of Li₂O/CaO

Figure 3 shows the effect of the relative percentage of the ratio of $\text{Li}_2\text{O}/\text{CaO}$ on the free volume size (V_0 -ps) measurements of the prepared samples. Similar to what have been seen from fluctuation in the glass indices, a fluctuation in the free volume size is recorded as ratio of $\text{Li}_2\text{O}/\text{CaO}$ increases. In comparison to sample 1 where the ratio of $\text{Li}_2\text{O}/\text{CaO} = 25\%$, an increase in the free volume size is observed at $\text{Li}_2\text{O}/\text{CaO} = 50\%$ (sample 2). The recorded increase in free volume size may be attributed to the location of positrons in the surrounding of an increased number of NBO bonds. The addition of Li_2O where $\text{Li}_2\text{O}/\text{CaO} = 75\%$ (sample 3) causes a significant decrease in the free volume size with lower intensity I_2 . The recorded increase in the intensity for sample 4 indicates the increase in the concentration of NBOs with the increase in the ratio of $\text{Li}_2\text{O}/\text{CaO} = 100\%$ with zero CaO content.

The formation of one MO_4 tetrahedron requires an additional oxygen atom or two single bonded oxygen ions. It can be provided by an alkali molecule such as Li_2O due to its ionic property [44]. The boric oxide is built up of BO_3 triangles and upon adding divalent oxides, such as CaO , the coordination number of the boron changes from SP^3 tetrahedral BO_4 to from SP^2 planar BO_3 , preserving the B–O bonding without the creation of non-bridging oxygen ions [8].

So the introduction of divalent oxides (CaO) causes a significant formation of the BO_3 groups with a lower coordination number, pursuing an equilibrium reaction $\text{BO}_{3/2} \leftrightarrow \text{BO}_{4/2} + \text{NBO}$. When the divalent ions are present in amounts greater than the number of the interstices available, they will act partly as bridges between the adjacent BO_4 tetrahedral. The CaO ions will thus become enclosed in the structural interstices or will act as bridges between the network forming units.

Furthermore, the average coordination number and molar volume are strongly correlated [45]. Therefore, it is expected that, with the insertion of Li_2O instead of CaO a transformation of a part of BO_3 groups into BO_4 structural unit will take place as it will be seen through the FT-IR measurements. It produces an assured increase in the number of nonbridging oxygen bonds (NBO) relative to the bridging bonds (BO). According to Sun [46], the single bond strength of B–O bond is 498 kJ/mol for BO_3 structural unit and 373 kJ/mol for BO_4 structural unit. It also means the replacement of strong oxygen linkages triangular units $\text{BO}_{3/2}$ by weaker anionic tetrahedral unit linkages $\text{BO}_{4/2}$. Thus, the fluctuation in NBO relative density manifests itself clearly by the periodic variation in the glass molar volume and hence the calculated free volume size.

FT-IR Structure Analysis

Fourier transform infrared spectroscopy (FTIR) is a technique for collecting and analyzing the obtained IR spectra. The role of the mixed alkali effect on the NBO_s/BO_s ratio is found out by analysis of FTIR spectroscopy and positron annihilation spectroscopy. It is also noted the influence of these modifier ions on the structural disorder of the glass matrix. Boron oxygen network can be in the form of planar BO_3 and/or tetrahedral BO_4 .

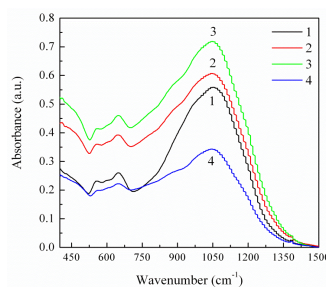


Figure 4: FT-IR Spectra of the different Investigated Glass Compositions

As shown in Fig. 4, the absorption bands are assigned for different stretching and bending vibrations like specific vibrations of B-O-B bending vibrations, O₃B-O-BO₄ bending vibrations, B-O stretching vibration of BO₄ units in tri-, tetra- and penta- borate groups, B-O stretching vibration of trigonal BO₃ units in boroxol rings, B-O stretching vibrations of BO₃ units in metaborate, pyroborate and orthoborate groups and specific vibrations of B-O-B bending vibrations. The role of the modifier ions (Li₂O and CaO) on the BO₄/BO₃ ratio is found out by FTIR analysis. It is also noted the influence of these modifier ions on the structural disorder of the glass matrix. The results of Infrared absorption spectra of the investigated borophosphate glasses in the range extended from 1400 to 400 cm⁻¹ can be discussed as follow:

- Boron has three vibrational absorption bands at 1200-1600, 800-1200 and at 700 cm⁻¹.
- Planar BO₃ gives four fundamental bands around 950, 750, 1250 and 600 cm⁻¹.
- Tetrahedral BO₄ unit also gives four bands around 1000, 900, 600, 550 cm⁻¹.
- The broad and strong band appeared at 1020-1030 cm⁻¹ is due to BO₄ tetrahedra.
- The strong band at 700 cm⁻¹ is due to the bending vibration of B-O-B linkages of BO₃ units [47, 48].
- The weak band observed at 520 cm⁻¹ is due to vibration of BO₄ tetrahedra.
- It could be concluded that the introduction of Li₂O transforms some of the BO₃ triangles to BO₄ tetrahedra with the formation of non-bridging oxygen atoms.
- Furthermore, infrared absorption bands of vibration mode P=O superposed with (PO₂)_{as} mode are observed with band assigned to (P-O⁻)_{as} vibration in Q² (1097 cm⁻¹) [49, 50].
- It is also attributed to vibration of Q⁰ tetrahedra at 1017 cm⁻¹ [51-53] and to deformation mode of P-O⁻ groups (530 cm⁻¹) [54], respectively.
- With increasing Li₂O on the expense of CaO, the appearance of the band at nearly 913-937 cm⁻¹ is an indication of the presence of (P-O-P) as bridging oxygen bonds (BOs).
- Appearance of the band at 1045 cm⁻¹ with increasing Li₂O proves that the Q⁰ tetrahedron exists.
- Disappearances of the band at 990 cm⁻¹ indicates that Q¹ structure units are decreased.
- So the structure of phosphate network approaches to metaphosphates with mainly Q² structural unit.
- When Li₂O is present in larger quantities the π -bond of P=O may be ruptured with the creation of non-bridging oxygen ions.
- Addition of an alkali oxide shifts the reaction $Q^2 \rightarrow 2Q^1 + Q^0$ to the right direction. Substitution of Li₂O with CaO depolymerizes the phosphate glass network by systematic conversion of Q² structural units into Q¹ structural units [55].
- Conversion Q² to Q¹ is taking place due to breaking P-O-P linkages.
- For further addition of Li₂O, Q¹ structural units get converted into Q⁰ structural units and glass network becomes more depolymerized.

- Addition of Li_2O to phosphate glass in the expense of CaO can decrease the cross-links between phosphate chains [56]. As alkali ion Li_2O increases it can lead to the breaking of P-O-P linkages and the creation of non-bridging oxygen atoms in the glass [57].
- Increasing the creation of non-bridging oxygens increases the polarization and hence the glass reflectance, R .
- The spectra of indicate that there is no evidence for the presence of characteristic bands of Fe_2O_3 .
- According to a proposed model [58] the vibrations for Fe^{2+} ions should be at 230 cm^{-1} and for Fe^{3+} ions should be at 290 cm^{-1} .
- Furthermore, Mössbauer measurements [59] suggested that, Fe^{2+} and Fe^{3+} ions occupy sites with octahedral or distorted octahedral coordination without participation in the host glass network giving the reason for absent of absorption bands of Fe–O vibrations.
- It concludes that, vibration of Fe–O may appear below 300 cm^{-1} or the band for the Fe–O vibrations may have superimposed or masked with the vibration of O=P–O linkage [60].

CONCLUSIONS

Mixed alkali effect has proven its ability to change the structure and optical properties of alkali borophosphate glasses containing Fe_2O_3 . The increase in molar percentage of the ratio $\text{Li}_2\text{O}/\text{CaO}$ induced a periodic change in the ratio of NBO/BO. Such change in the NBO/BO stimulates a similar change in the glass refractive indices and available free volume. The considerable molar and oxide ion polarizabilities of NBO are the motivation for the obtained increase in refractive index value. Furthermore, adjusting the ratio of NBO/BO through the alteration in $\text{Li}_2\text{O}/\text{CaO}$ leads to a variation in the glass free volume size associated with the change in the glass molar volume.

REFERENCES

1. S. G. Kosinski, D. M. Krol, T. M. Duncan, D. C. Doglass, J. B. MacChesney, J. R. Simpson, J. Non-Cryst. Solids 105 (1988) 45–52.
2. R. K. Brow, “Review: the structure of simple phosphate glasses,” J. Non-Cryst. Solids 263-264 (2000) 1–28.
3. N. H. Ray, Inorganic Polymers (Academic Press, London, 1978) pp. 79-90.
4. J. F. Duce, J. J. Videau, and M. Couzi, “Structural Study of Borophosphate Glassed by Raman and Infrared Spectroscopy,” Phys. Chem. Glasses 34 (1993) 212–218.
5. J. F. Duce and J. J. Videau, “Physical and chemical characterizations of sodium borophosphate glasses,” Mat. Lett. 13 (1992) 271-274.
6. L. Koudelka, and P. Močsner, “Borophosph glasses of the $\text{ZnO-B}_2\text{O}_3\text{-P}_2\text{O}_5$ system,” Mater. Lett. 42 (2000) 194-199.
7. M. Abdel-Baki, F. A. Abdel Wahab, A. Radi, and F. El-Diasty, “Factors affecting optical dispersion in borate glass systems,” J. Phys. Chem. Solids 68 (2007) 1457-1470.
8. M. Abdel-Baki, and F. El-Diasty, “Role of oxygen on the optical properties of borate glass doped with ZnO ,” J.

- Solid State Chem. 43 (2011) 2762-2769.
9. M. Abdel-Baki, and F. El-Diasty, "Glasses for photonic technologies," Int. J. Opt. Appl. 3 (2013) 125-137.
 10. F. El-Diasty, M. Abdel-Baki, F. A. Abdel Wahab, "Tuned intensity-dependent refractive index n_2 and two-photon absorption in oxide glasses: role of non-bridging oxygen bonds in optical nonlinearity," Opt. Mater. 31 (2008) 161-166.
 11. F. El-Diasty, M. Abdel-Baki, A. M. Bakry, "Resonant-type third-order optical nonlinearity and optical bandgap in multicomponent oxide glasses," Appl. Opt. 48 (2009) 2444-2449.
 12. E. M. Dianov, M. V. Grekov, I. A. Bufetov, S. A. Vasiliev, O. I. Medvedkov, V. G. Plotnichenko, V. V. Koltashev, A. V. Belov, M. M. Bubnov, S. L. Semjonov, and A. M. Prokhorov, "CW high power 1.24 μ m and 1.48 μ m Raman lasers based on low loss phosphate fibre," Electron. Lett., 33 (1997) 1542-1544.
 13. L. Petit, T. Cardinal, J. J. Videau, F. Smektala, T. Jouan, K. Richardson, and A. Schulte, "Fabrication and characterization of new Er³⁺ doped niobium borophosphate glass fiber," Mater. Sci. Eng. B 117 (2005) 283-286.
 14. T. Cardinal, E. Fargin, G. Le Flem, and S. Leboiteux, "Correlations between structural properties of Nb₂O₅-NaPO₃-Na₂B₄O₇ glasses and non-linear optical activities," J. Non-Cryst. Solids 222 (1997) 228-234.
 15. M. Dussauze, O. Bidault, E. Fargin, M. Maglione, and V. Rodriguez, "Dielectric relaxation induced by a space charge in poled glasses for nonlinear optics," J. Appl. Phys. 100 (2006) 034905-7.
 16. H. Takebe, Y. Baba, M. Kuwabara, J. Non-Cryst. Solids 352 (2006) 3088-3094.
 17. J. F. Duce, J. J. Videau, Matter Lett. 13 (1992) 271-274.
 18. S. Gu, Z. Wang, S. Jiang, H. Lin, "Influences of Fe₂O₃ on the structure and properties of Bi₂O₃-B₂O₃-SiO₂ low-melting glasses," Ceram. Int. 40 (2014) 7643-7645
 19. P. A. Bingham, R. J. Hand, S. D. Forder, "Doping of iron phosphate glasses with Al₂O₃, SiO₂ or B₂O₃ for improved thermal stability," Mater. Res. Bull. 41 (2006) 1622-1630.
 20. A. Mogus-Milankovic, A. Santic, A. Gajovic, D. E. Day, J. Non-Cryst. Solids 325 (2003) 76-84.
 21. D. W. Collins, L. N. Mulay, J. Am. Ceram. Soc. 54 (1971) 69.
 22. H. Akamatsu, K. Fujita, S. Murai, K. Tanaka, "Magneto-optical properties of transparent divalent iron phosphate glasses," Appl. Phys. Lett. 92 (2008) 251908.
 23. S. Kabi, A. Ghosh, EPL - Europhys. Lett. 100 (2012) 26007.
 24. R. K. Singh, G. P. Kothiyal, A. Srinivasan, "Electron spin resonance and magnetic studies on CaO-SiO₂-P₂O₅-Na₂O-Fe₂O₃ glasses," J. Non-Cryst. Solids 354 (2008) 3166-3170.
 25. L. Ma, R. K. Brow, A. Choudhury, "Structural study of Na₂O-FeO-Fe₂O₃-P₂O₅ glasses by Raman and Mössbauer spectroscopy," J. Non-Cryst. Solids 402 (2014) 64-73.
 26. E. Mansour, "Mixed alkali effect in quaternary K₂O-Li₂O-BaO-B₂O₃ glasses containing V₂O₅," Physica B 362 (2005) 88-94.

27. M. A. Khashan, A. M. El-Naggar, "A new method of finding the optical constants of a solid from the reflectance and transmittance spectrograms of its slab," *Opt. Commun.* 174 (2000) 445-453.
28. 1- P. Kirkegaard, M. Eldrup, O. E. Mogensen and N. Pedersen, "Program system for analysing positron lifetime spectra and angular correlation curves," *Comput. Phys. Commun.* 23 (1981) 307-335 (PATFIT 88, 1988 version).
29. A. T. Stewart and L. Roellig, Ed. "Positron Annihilation", Academic Press, New York, 1967, p. 438.
30. V. I. Goldanski, *Atomic Energy Rev.*, 6 (1968) 1-148.
31. A. Marotta, A. Buri, F. Branda, P. Pernice, A. Aronne, "Structure and devitrification behaviour of sodium, lithium and barium borophosphate glasses," *J. Non-Cryst. Solids* 95-96 (1987) 593-599.
32. M. Born, E. Wolf, "Principle of Optics, Pergamon Press 1984.
33. J. A. Duffy, "The electronic polarizability of oxygen in glass and effect of composition," *J. Non-Cryst. Solids* 297 (2002) 275-284.
34. J. A. Duffy, M. D. Ingram, in: D. Uhlman, N. Kreidl (Eds.), *Optical Properties of Glass*, American Ceramic Society, Westerville, 1991.
35. V. Dimitrov, T. Komatsu, "An interpretation of optical properties of oxides and oxides glasses in terms of the electronic polarizability and average single bond strength (review)," *J. Univ. Chem. Technol. Metal.* 45 (2010) 129-250.
36. J. A. Duffy, "Electronic polarisability and related properties of the oxide ion," *Phys. Chem. Glasses* 30 (1989) 1-4.
37. N. Jiang, *Solid State Commun.* 122 (2002) 7.
38. A. Abou Shama, M. S. Abd El Keriem, M. Abdel-Baki, F. El-Diasty, "RDF analysis, Positron Annihilation and Raman Spectroscopy of $x\text{TiO}_2-(60-x)\text{SiO}_2-40\text{Na}_2\text{O}$ nonlinear optical glasses: III. Non-bridging oxygen bonds tracing and structure analysis," *J. Non-Cryst. Solids* 353 (2007) 2708-2716.
39. P. Hautojarvi and C. Corbel, "Positron Spectroscopy of Solids," Eds. A. Dupasquier, A. P. Mills Jr, IOS Press, Amsterdam, 1995.
40. S. Seeger and F. Banhart, *Phys. Stat. Sol.* 102 (1987) 171.
41. O. E. Morgensen, "Positron Annihilation in Chemistry," Springer-Verlag, Berlin, 1995.
42. S. J. Tao, Positronium annihilation in molecular substances. *J. Chem. Phys.* 56 (1972) 5499-5510.
43. Nakanishi, H., Wang, S. J., Jean, Y. C., 1988. In: Sharama, S. C. (Ed.), *Positron Annihilation Studies of Fluids*. World Scientific, Singapore, (1988) 292-298.
44. S. R Langhoff and C. W. Bauschlicher, Jr., "Theoretical study of the diatomic alkali and alkaline-earth oxides," *J. Chem. Phys.* 84 (1986) 4474-4480.
45. F. A. Moustafa, M. Abdel-Baki, A. M. Fayad, F. El-Diasty, "Role of mixed valence effect and orbital hybridization on molar volume of heavy metal glass for ionic conduction pathways augmentation," *Am. J. Mater.*

- Sci. 4 (2014) 119-126.
46. K. H. Sun, J. Am. Ceram. Soc. 30 (1947) 277.
47. G. Sharma, K. S. Manupriya, S. Mohan, H. Singh, S. Bindra, Radiat. Phys. Chem. 75 (2006) 959-966.
48. E. R Shaaban, M. shapaan, Y. B. Saddeek, J. Phys. Cond. Mater. 20 (2008) 155/08.
49. H. S. Liu, T. S. Chin, S. W. Yung, "FTIR and XPS studies of low-melting PbO - ZnO - P_2O_5 glasses," Mater. Chem. Phys. 50 (1997) 1-10.
50. J. C. Hurt, C. J. Phillips, "Structural role of zinc oxide in glasses in the system Na_2O - ZnO - SiO_2 ," J. Am. Ceram. Soc. 53 (1970) 269-273.
51. R. K. Brow, "Review: the structure of simple phosphate glasses," J. Non-Cryst. Solids 263-264 (2000) 1-28.
52. G. L. Saout, F. Fayon, C. Bessada, P. Simon, A. Blion, Y. Vaills, "A multispectroscopic study of $PbO_xZnO_{0.6-x}(P_2O_5)_{0.4}$ glasses," J. Non-Cryst. Solids 293/295 (2001) 657-662.
53. R. K. Brow, D. R. Tallant, S. T. Myers, C. C. Phifer, "The short-range structure of zinc polyphosphate glass," J. Non-Cryst. Solids 191(1995) 45-55.
54. D. E. Corbridge, "Infra-red analysis of phosphorus compounds," J. Appl. Chem. 6 (1956) 456-465.
55. S. Ibrahim, M. Abdel-Baki and F. El-Diasty, "Zinc borophosphate glasses for infrared-based optical applications," Opt. Eng. 51 (2012) 093401-7.
56. A. A. Higazy, B. Bridge, A. Hussein, M. A. Ewaida, "Elastic Constants and Structure of the Vitreous System ZnO - P_2O_5 " J. Acoustical Soc. Am. 86 (1989) 1453-1458.
57. Y. M. Moustafa, K. El-Egili, "Infrared Spectra of Sodium Phosphate Glasses," J. Non-Crystal Solids 240 (1998) 144-153.
58. B. N. Nelson and G. J. Exarhos, J. Chem. Phys. 71 (1979) 2739.
59. C. S. Ray, X. Fang, M. Karabulut, G. K. Marasinghe, D. E. Day, J. Non-Cryst. Solids 249 (1999) 1.
60. Y. M. Moustafa, K. El-Egili, H. Doweidar, I. Abbas, "Structure and electric conduction of Fe_2O_3 - P_2O_5 glasses," Physica B 353 (2004) 82-91.

